Springer Series in Advanced Microelectronics 38

Thorsten Hehn
Yiannos Manoli

CMOS Circuits for Piezoelectric Energy Harvesters

Efficient Power Extraction, Interface Modeling and Loss Analysis

Springer

Springer Series in Advanced Microelectronics

Volume 38

The Springer Series in Advanced Microelectronics provides systematic information on all the topics relevant for the design, processing, and manufacturing of microelectronic devices. The books, each prepared by leading researchers or engineers in their fields, cover the basic and advanced aspects of topics such as wafer processing, materials, device design, device technologies, circuit design, VLSI implementation, and subsystem technology. The series forms a bridge between physics and engineering and the volumes will appeal to practicing engineers as well as research scientists.

More information about this series at http://www.springer.com/series/4076

Thorsten Hehn · Yiannos Manoli

CMOS Circuits for Piezoelectric Energy Harvesters

Efficient Power Extraction, Interface Modeling and Loss Analysis

Springer

Thorsten Hehn
HSG-IMIT–Institute of Micromachining and Information Technology
Villingen-Schwenningen
Germany

Yiannos Manoli
Fritz Huettinger Chair of Microelectronics, Department of Microsystems Engineering
University of Freiburg–IMTEK
Freiburg
Germany

ISSN 1437-0387 ISSN 2197-6643 (electronic)
ISBN 978-94-017-9287-5 ISBN 978-94-017-9288-2 (eBook)
DOI 10.1007/978-94-017-9288-2

Library of Congress Control Number: 2014944326

Springer Dordrecht Heidelberg New York London

Printed on acid-free paper

Springer is part of Springer Science+Business Media (www.springer.com)

Preface

This book deals with the challenge of exploiting ambient vibrational energy, which can be used to power small and low-power electronic devices, e.g., wireless sensor nodes. Generally, particularly for low voltage amplitudes, low-loss rectification is required to achieve high conversion efficiency. In the special case of piezoelectric energy harvesting, pulsed charge extraction has the potential to extract more power compared to a full-bridge rectifier. Therefore, a fully autonomous CMOS integrated interface circuit for piezoelectric generators which fulfills these requirements is presented. This book covers three main aspects of the integrated interface circuit:

First of all, the book explains in detail the different circuit blocks on transistor level and highlights techniques to reduce the power consumption. Hence, only a very small fraction of the power delivered by the generator is wasted, which is extremely important in order to achieve a high overall harvesting efficiency, especially in case the piezoelectric generator outputs little power.

Second, the book analyzes the various loss mechanisms within the CMOS chip, such as conduction losses, switching losses, etc. Therefore, a mathematical method of approximating the conduction losses is presented, which reduces calculation effort and gives deep insight into the loss dependency on different parameters. A detailed breakdown of the actual chip losses identifies the most dominant loss mechanisms and gives ideas how these losses can be further reduced.

Third, since the performance of the CMOS chip strongly depends on the used power source, lot of effort is spent on investigating the interaction between the interface circuit and the piezoelectric generator. For accurate simulations, a model which takes into account this electromechanical feedback is used. A CMOS chip has been fabricated and tested under laboratory conditions in combination with one custom-made and one commercially available piezoelectric generator. By comparing measurement and simulation results, the used model could be verified.

The presented CMOS chip has been shown to be fully autonomous and self-powered down to a piezoelectric output power in the range of 10 μW. It enables cold-startup and enhances the extracted power compared to the commonly known diode rectifiers by up to 127 %, depending on the excitation conditions. For low excitations, due to the boosting effect, the chip harvests power where a diode rectifier would harvest nothing. The chip operates properly for piezoelectric voltage amplitudes in the range of 1.3–20 V and for excitation frequencies from 50 Hz to 2 kHz.

Due to these key properties enabling universal usage, other CMOS designers working in the field of energy harvesting will be encouraged to use some of the shown structures for their own implementations. The book highlights the design process from scratch to the final chip. Therefore, it gives the designer a comprehensive guide of how to

- setup an appropriate harvester model to get realistic simulation results,
- design the integrated circuits for low power operation,
- setup a laboratory measurement environment in order to extensively characterize the chip in combination with the real harvester,
- and finally interpret the simulation and measurement results in order to improve the chip performance.

Since the dimensions of all devices (transistors, resistors etc.) are given, readers and other designers can easily re-use the presented circuit concepts.

Villingen-Schwenningen, Germany Thorsten Hehn
Freiburg, Germany Yiannos Manoli

Acknowledgments

The writing of this book has been one of the most significant academic challenges I have ever had to face. Without the support, patience and guidance of the following people, this study would not have been completed.

First of all, I would like to express my deepest appreciation to my advisor and head of the Fritz Huettinger chair of Microelectronics, Prof. Yiannos Manoli, for providing me with an excellent atmosphere for doing research and to finally do my Ph.D. at his chair. He has always taken his time to listen to my problems and questions, often leading to lively discussions, which helped me improving my research work.

For the first three years of my time spent at the chair, the graduate program *Micro Energy Harvesting*, funded by the Deutsche Forschungsgemeinschaft (DFG) under grant number 1322, offered me the opportunity to really focus on my research. I want to express a thank to the DFG for giving me financial support, and to the whole community, including all the other doctoral candidates and their supervisors, for the pleasant atmosphere during the regular seminars and their willingness for supporting me. The speaker of the graduate program, Prof. Peter Woias, has always shown interest in my work and has given valuable tips. Thank you.

Toward the end of my time in the graduate program, I had a great time with Dr. Christoph Eichhorn developing a joint demonstrator, which shows the performance of both the tunability of piezoelectric generators (Eichhorn's part) and the improvement of extracted power (my part). Many thanks for the fruitful and pleasant collaboration.

Another special thank goes to the former members of the Energy Harvesting group at the chair, Dr. Christian Peters and Dr. Dominic Maurath, who guided me especially during the initial phase of my research. They were always available for talking about any of my concerns when I was stuck, which oftentimes helped me finding clever solutions to many problems.

With his profound analytical mathematical skills, Friedrich Hagedorn established a basis for my work during the period when he worked for his student research project under my supervision. He introduced the idea of the improved switching technique and derived large parts of the mathematical theory shown in Chap. 4. I want to thank him for this invaluable contribution to my work.

During the everyday life of a (micro-)electronic circuit designer, problems regarding the circuit or the simulation/lay outing software are a daily occurrence. I would like to express my gratitude to Matthias Kuhl, Christian Moranz, Michael Maurer, Markus Kuderer, Stanis Trendelenburg, Armin Taschwer, and Rolf Schlecker, who always helped me solving my problems whenever they appeared.

Finally, I gratefully thank my family, especially my parents Ute and Roland and my sister Sabine, for providing me with the environment that enabled me to totally focus on my work. It would not have been possible to complete my research work without their help.

Contents

Nomenclature

Abbreviations

AC	Alternating Current
BAN	Body Area Network
BG	Bias Generator
CLCC	Ceramic Lead Chip Carrier
CMOS	Complementary Metal-Oxide Semiconductor
DC	Direct Current
EMG	Electromyogram
GEMC	Generalized Electromechanical Coupling Factor
GSM	Global System for Mobile Communications
HVAC	Heating, Ventilation, and Air-Conditioning
MEMS	Micro-Electro-Mechanical System
MPP	Maximum Power Point
MPPT	Maximum Power Point Tracking
MOSFET	Metal-Oxide Semiconductor Field Effect Transistor
NMOS	N-Channel MOSFET
NVC	Negative Voltage Converter
PCB	Printed Circuit Board
PMOS	P-Channel MOSFET
PSCE	Pulsed-Resonant Charge Extractor
PZT	Lead Circonate Titanate
RCD	Reverse Current Detector
RFID	Radio Frequency Identification
SECE	Synchronous Electric Charge Extraction
SSHI	Synchronous Switch Harvesting on Inductors
WLAN	Wireless Local Area Network
WSN	Wireless Sensor Node
ZCD	Zero Crossing Detector

Symbols

$a(t)$	$= \ddot{y}(t)$ Acceleration of the external vibration (m/s^2)
$\hat{a}$	Amplitude of $a(t)$ (m/s^2)
η	Efficiency variable
η_{ab}	Numerically solved efficiency of SECE*ab*, where $ab \in \{12,13,23\}$(–)
η_{abcd}	Numerically solved efficiency of combined SECE*abcd*, where $abcd \in \{1223,1323\}$ (–)
$\eta_{ab,\mathrm{lin}}$	Approximated efficiency of SECE*ab*, where $ab \in \{12,13,23\}$ (–)
$\eta_{abcd,\mathrm{lin}}$	Approximated efficiency of SECE*abcd*, where $abcd \in \{1223,1323\}$ (–)
η_{chip}	$\frac{P_{\mathrm{PSCE,out}}}{P_{\mathrm{PSCE,in}}}$ Efficiency of the PSCE chip (–)
η_{harv}	$\frac{P_{\mathrm{PSCE,out}}}{P_{\mathrm{lim}}}$ Harvesting efficiency of the PSCE chip, referred to the absolute maximum power P_{lim} (–)
$\Delta\eta_{abcd}$	Numerically solved efficiency improvement of SECE*abcd*, where $abcd \in \{1223,1323\}$, referred to SECE13 (–)
$\Delta\eta_{abcd,\mathrm{lin}}$	Approximated efficiency improvement of SECE*abcd*, where $abcd \in \{1223,1323\}$, referred to SECE13 (–)
C	Capacitance variable (F)
C_{buf}	Storage buffer capacitance (F)
C_{mc}	Lumped mechanical capacitance in the coupled piezoelectric harvester model (F)
C_P	Piezoelectric output capacitance (F)
d	Parasitic damping (Ns/m)
d_e	Electrical damping due to load (Ns/m)
E	Electrical energy variable (Ws)
E_{P0}	Energy stored in C_P at $t= t_0$ (Ws)
E_W	Energy loss (Ws)
E_{Wab}	Numerically solved energy loss of SECE*ab*, where $ab \in \{12,13,23\}$ (Ws)
$E_{Wab,\mathrm{lin}}$	Approximated energy loss of SECE*ab*, where $ab \in \{12,13,23\}$ (Ws)
f_{oc}	Resonant frequency of the open-circuited structure (Hz)
f_{sc}	Resonant frequency of the short-circuited structure (Hz)
F_e	Restoring force due to transducer feedback (N)
$\mathbf{f}_n$	State equation of switch configuration $n \in \{1,2,3\}$
$\mathbf{F}_n$	Solution of $\mathbf{f}_n$
GND	= 0 V Ground potential (V)
Γ	Generalized electromechanical coupling factor (GEMC) (As/m)
$\Gamma^2_{\mathrm{res,opt}}$	Optimum squared GEMC necessary to achieve maximum output power using resistor load (As/m)
$\Gamma^2_{\mathrm{rect,opt}}$	Optimum squared GEMC necessary to achieve maximum output power using rectifier-capacitor load (As/m)
$\Gamma^2_{\mathrm{rect,border}}$	Squared GEMC indicating the border between the regimes showing one and two output power extrema, using rectifier-capacitor load (As/m)

$\Gamma^2_{\mathrm{SECE,opt}}$	Optimum squared GEMC necessary to achieve maximum output power using SECE load (As/m)
$\Gamma^2_{\mathrm{cross}}$	Squared GEMC where the output power using the rectifier-capacitor load and the SECE load are equal (As/m)
I	Electrical current variable (A)
I_{buf}	Electrical current flowing into the buffer capacitor (A)
I_L	Electrical current flowing through the external SECE inductor (A)
I_{L0}	= 0 Electrical current flowing at the initial instant of the transfer process (A)
I_{Lab}	I_L flowing during SECEab, where $ab \in \{12,13,23\}$ (A)
k^2_{eff}	Squared effective coupling factor of the harvester structure (–)
k	$= k_P + k_S$ Sum of the stiffness values of the piezoelectric material and the mechanical spring (N/m)
k_{13}	Coupling factor of the piezoelectric material (–)
k_P	Stiffness of the piezoelectric material (N/m)
k_S	Stiffness of the mechanical spring (N/m)
L	External SECE inductance (H)
L_{mc}	Lumped mechanical inductance in the coupled piezoelectric harvester model (H)
m	Total effective mass of the harvester (kg)
ω	$= 2\pi f$ Angular frequency of the external vibration (rad/s)
ω_0	$:= \frac{1}{\sqrt{LC_P}}$ Commonly used abbreviation (rad/s)
ω_{oc}	$= 2\pi\, f_{\mathrm{oc}}$ Angular resonant frequency of the open-circuited structure (rad/s)
ω_{sc}	$= 2\pi\, f_{\mathrm{sc}}$ Angular resonant frequency of the short-circuited structure (rad/s)
ω_n	$= \sqrt{\frac{k}{m}}$ Angular natural frequency of the mechanical system (rad/s)
$p_{a,ab}$	$= \int_{t_0}^{t_{ab}} I^2_{Lab}(t)\mathrm{d}t$ Commonly used abbreviation, where $ab \in \{12,13,23\}$ ($\mathrm{A^2 s}$)
$p_{b,ab}$	$= \int_{t_{ab}}^{t_{Eab}} I^2_{Lab}(t)\mathrm{d}t$ Commonly used abbreviation, where $ab \in \{12,13,23\}$ ($\mathrm{A^2 s}$)
P	Electrical power variable (W)
$P_{\mathrm{act,dyn}}$	Dynamic power consumption of the control circuitry (W)
$P_{\mathrm{act,stat}}$	Static power consumption of the control circuitry (W)
P_{cond}	Conduction loss due to parasitic series resistance (W)
P_{cross}	Cross current loss of the digital circuitry (W)
P_{dc}	Conduction loss of the external inductor (W)
P_{harv}	Harvested power (W)
P_{lim}	Absolute maximum harvester output power (W)
P_{NVC}	$= P_{\mathrm{NVC,act}} + P_{\mathrm{NVC,pass}}$ Conduction loss due to the parasitic series resistance of the NVC (W)
$P_{\mathrm{NVC,act}}$	Conduction loss due to the parasitic series resistance of the active NVC (W)

$P_{\mathrm{NVC,pass}}$	Conduction loss due to the parasitic series resistance of the passive NVC (W)
$P_{\mathrm{PSCE,in}}$	Power flowing into the PSCE chip (W)
$P_{\mathrm{PSCE,out}}$	Power flowing out of the PSCE chip (W)
P_{rect}	Piezoelectric output power using rectifier load (W)
$P_{\mathrm{rect,max}}$	Piezoelectric output power using rectifier load at optimum load resistance (W)
P_{res}	Piezoelectric output power using resistive load (W)
$P_{\mathrm{res,max}}$	Piezoelectric output power using optimum resistive load (W)
P_{SECE}	Piezoelectric output power using SECE load (W)
$P_{\mathrm{SECE,max}}$	Piezoelectric output power using SECE load, assuming optimal electromechanical coupling (W)
$P_{\mathrm{S}a}$	Conduction loss due to parasitic series resistance of the switch S_a where $a \in \{1,2,3\}$ (W)
P_W	Power loss (W)
Q	Quality factor of parasitic damping (–)
Q_e	Quality factor of electrical damping (–)
$[P,R]^R$	Output power/load resistance for resonant excitation (W,Ω)
$[P,R]^{OR}$	Output power/load resistance for off-resonant excitation (W,Ω)
R_{buf}	Parasitic series resistance of the buffer capacitor (Ω)
R_{dc}	Parasitic series resistance of the external SECE inductor (Ω)
R_{mc}	Lumped mechanical resistance in the coupled piezoelectric harvester model (Ω)
R_{NVC}	Parasitic series resistance of the NVC (Ω)
R_{on}	MOSFET channel on-resistance (Ω)
$R_{\mathrm{rect,opt}}$	Optimal load resistance of the rectifier load (Ω)
$R_{\mathrm{res,opt}}$	Optimal load resistance (Ω)
R_{L}	Load resistance (Ω)
$R_{\mathrm{S}a}$	Parasitic series resistance of the switch S_a where $a \in \{1,2,3\}$ (Ω)
t	Time variable (s)
t_0	Time when transfer process starts (s)
t_E	Time when transfer process terminates (s)
t_{ab}	End of first phase of SECEab, where $ab \in \{12,13,23\}$ (s)
t_{Eab}	End of second phase of SECEab, where $ab \in \{12,13,23\}$ (s)
T	$=\frac{1}{f}$ Length of an excitation period (s)
V	Voltage variable (V)
V_{buf}	Voltage on the storage buffer capacitor (V)
$V_{\mathrm{buf,ss}}$	Steady-state buffer voltage (V)
V_{DD}	Supply voltage of the control circuitry (V)
$V_{\mathrm{DD,max}}$	$\max(V_{\mathrm{buf}}, V_{L-})$ High level of the control signal of switch S_2 (V)
V_{GS}	MOSFET gate-source voltage (V)
V_{L+}	Left terminal of the external inductor, connected to the NVC output (V)
V_{L-}	Right terminal of the external inductor (V)

V_{mc}	Lumped voltage source in the coupled piezoelectric harvester model (V)
V_P	$= V_{L+} - V_{L-}$ Voltage across the piezoelectric terminals (V)
$\hat{V}_P$	Amplitude of V_P (V)
$V_{P,\mathrm{oc}}$	Voltage across the piezoelectric terminals at open circuit (V)
$V_{P,\mathrm{PSCE}}$	Voltage across the piezoelectric terminals with PSCE load (V)
V_{P0}	$=\hat{V}_P$ Value of V_P at the beginning of the transfer process (V)
V_T	MOSFET threshold voltage (V)
W/L	MOSFET aspect ratio (m/m)
x	$:= \frac{V_{P0}}{V_{\mathrm{buf}}} = \frac{\hat{V}_P}{V_{\mathrm{buf}}}$ Commonly used abbreviation (–)
$y(t)$	Displacement of the harvester frame (m)
$\hat{y}$	Amplitude of $y(t)$ (m)
$z(t)$	Relative displacement of the seismic mass to the frame (m)
$\hat{z}$	Amplitude of $z(t)$ (m)
$\mathbf{z}$	$:= V_P\ I_L)$ Commonly used state vector (V A)
$\mathbf{z}_0$	$\mathbf{z}$ at $t = t_0$ (V A)
$\mathbf{z}_E$	$\mathbf{z}$ at $t = t_E$ (V A)
ζ_d	Dimensionless parasitic damping (–)
ζ_e	Dimensionless electrical damping (–)

Chapter 1
Introduction

In the last few years, energy harvesters have decreased in size, and at the same time increased their output power. These properties make energy harvesting attractive for powering wireless sensor nodes (WSNs) which are originally battery powered, with the goal of prolongating their lifetime. This chapter starts with a rough review of the main energy harvesting mechanisms, covering the thermoelectric, radio frequency (RF) and vibration based principles. For each mechanism, some representative application examples are shown, followed by possible applications of these conversion mechanisms in WSNs are presented. After that, a detailed review of the state of the art in interface circuits for vibration based energy harvesters is given. Therefore, the interface circuits are separated in two categories, one of them focusing on efficient AC/DC conversion, and the others incorporating impedance matching methods.

In order to classify the major achievements of the proposed interface circuit, a list of aspects which should be fulfilled when designing general interface circuitry for energy harvesters is given. Based on this list, the major achievements of this work are then discussed. This chapter ends up with a brief description of the organization of the book.

1.1 Energy Harvesting Principles

Energy harvesters[1] convert ambient energy into usable electrical energy. There are many possible conversion mechanisms, which are briefly presented in the following [49].

[1] Usually, the term *energy harvester* or *energy scavenger* is used for a microscale device converting small amounts of ambient energy into electrical energy. In the broader sense, such a device is of course a *generator*, and sometimes is referred to as a *converter* or a *transducer* as well. In this book, the terms *energy harvester* and *generator* are used as synonyms.

T. Hehn and Y. Manoli, *CMOS Circuits for Piezoelectric Energy Harvesters*,
Springer Series in Advanced Microelectronics 38, DOI 10.1007/978-94-017-9288-2_1

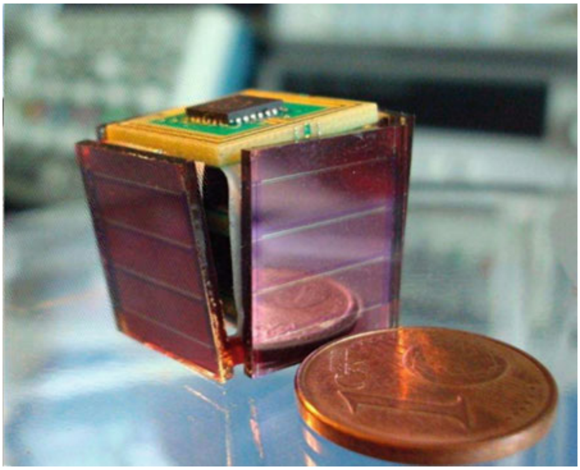

Fig. 1.1 Illustration of a sensor cube application integrating photovoltaic harvesters as packaging [34] (reproduced with kind permission of Valer Pop)

The probably most popular ambient energy source is sunlight which is converted into electrical energy by means of photovoltaic cells. Outdoors, they provide a power density of $100\,\mathrm{mW/cm^2}$, which reduces to $10-100\,\mu\mathrm{W/cm^2}$ for indoor application. Their efficiencies range from $5-30\,\%$, depending on the material used. Hence, power densities provided by photovoltaic cells usually are in the order of $10\,\mathrm{mW}$ outdoors and $10\,\mu\mathrm{W}$ indoors. Figure 1.1 shows a sensor cube powered by photovoltaic cells, providing $20\,\mu\mathrm{W}$ in indoor illuminating conditions.

Temperature gradients can also be converted into electrical energy, by exploiting the Seebeck effect: In case two ends of a piece of thermoelectric material are kept at a different temperature, i.e. a temperature gradient is present, an electrical voltage appears between the ends. A thermocouple made of two different materials and a metallic interconnect is the simplest thermoelectric generator. If several thermocouples are connected thermally in parallel and electrically in series, a thermogenerator with useable output voltage and power levels can be realized. The company Micropelt produces small-scale thermoelectric generators with a surface area of $14\,\mathrm{mm}^2$ and a thickness of $1\,\mathrm{mm}$, producing a matched power of $1.5\,\mathrm{mW}$ at $\Delta T = 10\,\mathrm{K}$ [29]. On one hand, these small generators allow the implementation of small WSNs which have a long lifetime and are reliable due to the absence of moving parts. But on the other hand, it is difficult to achieve a significant temperature gradient over the small thickness, requiring large heat sinks, increasing total system size. A photograph of Micropelt generator chips is depicted in Fig. 1.2.

Another possible source for energy harvesting are radio frequency (RF) waves available everywhere due to public telecommunication services like Global System for Mobile Communications (GSM) and Wireless Local Area Network (WLAN). This conversion mechanism exhibits relatively low power densities. For distances of

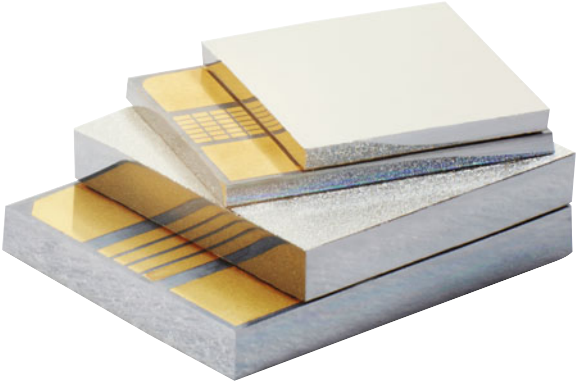

Fig. 1.2 Micropelt thermoelectric generator chip MPG-D751/MPG-D651 [29] (reproduced with kind permission of Micropelt)

Fig. 1.3 RF harvesting system with a small loop antenna (reproduced with kind permission of Tolgay Ungan)

$25 - 100\,\text{m}$ from a GSM base station, a power of $0.1 - 1\,\text{mW}/\text{m}^2$ may be achieved from single frequencies. WLAN exhibits one magnitude lower power densities [48]. Alternatively, a dedicated RF source can be positioned in front of a WSN in order to directly power this device at a small distance. Using this method, a transmission power of $200\,\mu\text{W}$ at a distance of $2\,\text{m}$ has been reported [46]. Figure 1.3 shows the corresponding RF system.

As a last conversion mechanism, harvesting energy from vibrations or motions is discussed in the following. For that purpose, mainly three conversion mechanisms exist: The capacitive [18, 52], the inductive [5, 41] and the piezoelectric [15, 20, 38] principle. The capacitive principle exploits the relative movement of two capacitor plates with respect to each other. This movement causes charges stored in the

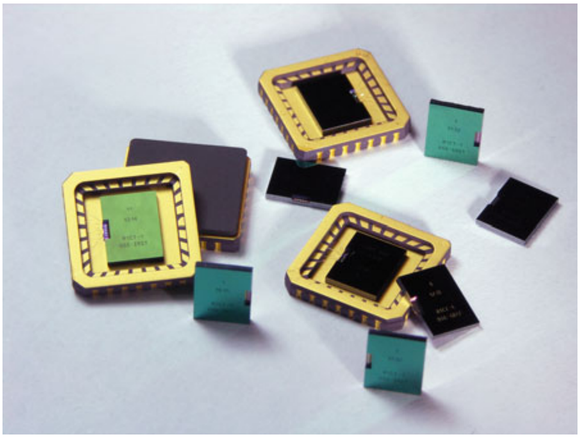

Fig. 1.4 Capacitive microgenerator chips, partly packaged in CLCC packages (reproduced with kind permission of Daniel Hoffmann)

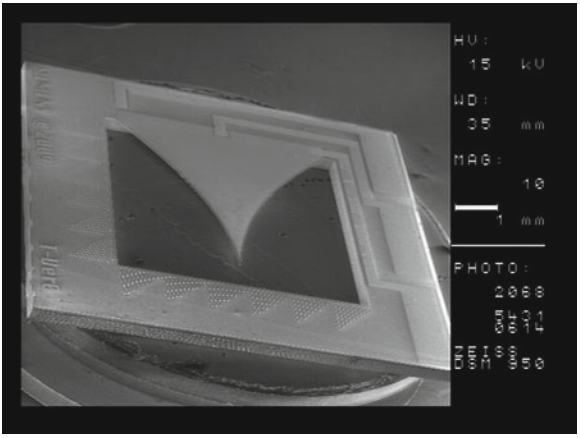

Fig. 1.5 SEM picture of a single triangular-curved piezoelectric cantilever which is an optimum for a uniform load (reproduced with kind permission of Ingo Kühne)

capacitor plates to be moved through an external load, producing electrical power. Figure 1.4 shows an example of a capacitive microgenerator packaged in a ceramic lead chip carrier (CLCC) package. For the inductive conversion principle, a permanent magnet moves relatively to a coil, inducing a voltage across the coil. Lastly, mechanical strain in a layer made of piezoelectric material produces a charge separation in the piezoelectric material which turns into a voltage between both surfaces of the layer. Figure 1.5 depicts a SEM image of a triangular-curved piezoelectric cantilever.

Each of the three main kinetic conversion principles (capacitive, inductive, piezoelectric) has its own advantages and disadvantages, which are summarized in the following [4, 40]:

- Compared to the other two principles, the capacitive conversion principle can be realized most easily in micro-electro-mechanical systems (MEMS) technology, and there exists a high level of corresponding process know-how. But unfortunately, capactive harvesters require an initial polarizing voltage or charge. This can be achieved by special materials called electrets which can provide the initial polarization and these can maintain their charge over several years [3]. Electrostatic harvesters suffer from a high output impedance, limiting the achievable output current. In contrast, the output voltage is usually very high (>100 V), posing a challenge in the interface circuit design. Parasitic capacitances within the structure can sometimes lead to reduced generator efficiency and cause capacitor electrodes shorting or sticking. Electrostatic generators exhibit by far the lowest energy storage density [40].
- The inductive conversion principle offers a well-established technique, with a variety of spring/mass configurations that can be used with various types of material. High-performance bulk magnets and multi-turn, macro-scale coils are readily available. A relatively high output current comes at the expense of a low output voltage (<1 V), requiring highly efficient rectifiers and boost converters to provide a voltage level suitable to supply common electronics. Problems exist in designing MEMS devices, due to the poor properties of planar magnets, the limited number of turns of planar coils, and the restricted vibration amplitude. The practical maximum energy density of inductive generators is much higher compared to capacitive generators, but lower than what is achieved by piezoelectric generators [40].
- The piezoelectric conversion principle offers the simplest approach, because there is no need for having complex geometries and numerous extra components. Vibrations are directly converted into electricity through the electroded piezoelectric material. Piezoelectric materials can be simply deposited using thin- and thick-film, hence it is well suited for MEMS processes. Piezoelectric harvesters are capable of producing relatively high output voltages but only at low electrical currents. Due to the fact that piezoelectric materials are strained directly, the piezoelectric properties limit overall performance and lifetime. The commonly used material lead circonate titanate (PZT) is very brittle and hence prone to crack if it is over-stressed. The piezoelectric conversion principle is discussed more detailed in Chap. 2. According to Roundy et al. [40], of the three kinetic conversion mechanisms, piezoelectric generators offer the highest practical maximum energy storage density.

According to [4, 39, 40], vibration-based energy harvesting is a viable means of obtaining the small quantities of energy necessary to power WSNs. The three main techniques of harvesting energy from ambient vibrations have been shown to be capable of generating output power levels in the range of a few microwatts to several hundred microwatts.